

Supporting Information for

In-depth Thermodynamic and Kinetic Analysis of Ethane Diffusion in ZIF-8

Bernd E. Schmidt^a, Pieter Cnudde^a, Veronique Van Speybroeck^{a*} and Louis Vanduyfhuys^{a*}

^aCenter for Molecular Modeling (CMM), Ghent University, Technologiepark 46, Zwijnaarde 9052, Belgium

* *Email:* veronique.vanspeybroeck@ugent.be; louis.vanduyfhuys@ugent.be

Contents

Supporting Information for	1
S1 Hopping model.....	2
S2 Force field and statistical ensemble validation	2
S3 Unraveling the free energy profile and its various contributions	3
S4 Temperature dependence	5
S5 Loading dependence	9
S5.1 Asymmetric	9
S5.2 Symmetric	13
REFERENCES	17

S1 Hopping model

The hopping model assumes that the diffusion process can be broken down into discrete hops on a 1D lattice. From this a hopping frequency (ν) can easily be introduced $\nu = \frac{\langle \text{number of successful hops} \rangle}{\text{time}}$. If we want to know the successful hops in one direction, ν needs to be divided by twice the number of dimensions, following the lattice random-walk theory. Next, only one-dimensional hops are considered, with this a time and position dependent hopping probability $p(x, t)$ can be determined which can be shown to satisfy the following diffusion equation:

$$\frac{\partial p(x, t)}{\partial t} = \frac{\nu \lambda^2}{2} \left[\frac{\partial^2 p(x, t)}{\partial x^2} \right]. \quad (1)$$

In equation 1, λ stands for the distance that is covered in each hop. From equation 1, the diffusion constant D can be identified as $D = \frac{\nu \lambda^2}{2}$. Finally, the above expression can be straightforwardly extended to d dimensions (still assuming no history dependency or memory effects):

$$D = \frac{\nu \lambda^2}{2d}. \quad (2)$$

S2 Force field and statistical ensemble validation

The NVT simulation with the Krokidas *et al.* FF¹ was also performed using the *ab-initio* optimized unit-cell. The resulting phenomenological free energy barrier is 44.8 kJ/mol and the self-diffusion coefficient is 3.37×10^{-14} m²/s, which differs by four orders of magnitude from the *ab-initio* results. This indicates that the initial cell parameters of the NVT simulation are vital when describing the diffusion of ethane in ZIF-8.

To analyze the impact of the transition state (TS) location on the phenomenological energy barrier and the resulting self-diffusion coefficient, a sensitivity analysis of the TS location is performed. For this, five different locations (α , β , γ , δ and ϵ) in the TS range are chosen, as is indicated in SI-Figure S1, and are used in the TST. The resulting phenomenological energy barriers and self-diffusion coefficients shown in SI-Table S1, where no impact of the TS location on these values can be seen.

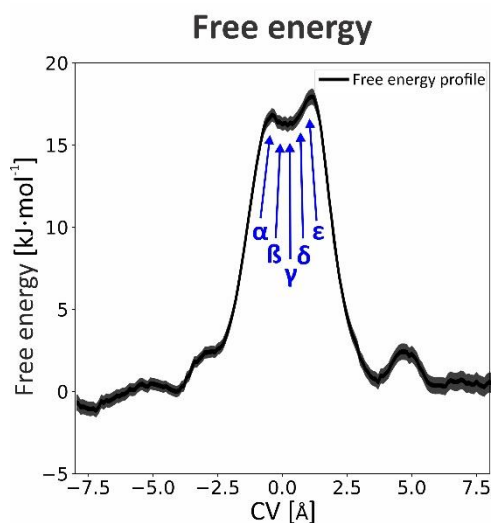


Figure S1: Free energy profile of the diffusion of ethane in ZIF-8 with the different locations used for the sensitivity analysis indicated.

Table S1: Phenomenological energy barriers according to transition state theory and corresponding diffusivities for diffusion of one ethane molecule in ZIF-8 using the Krokidas FF in the NPT ensemble (temperature of 300K and mechanical pressure of 1 bar). The phenomenological energy barriers and corresponding diffusivities are calculated with different transition state locations as indicated in SI-Figure S1.

	$\Delta G_{\text{phen}}^{\ddagger}$ (kJ/mol)	D_{self} (m ² /s)
α	30.71	1.08×10^{-11}
β	30.71	1.08×10^{-11}
γ	30.71	1.08×10^{-11}
δ	30.71	1.08×10^{-11}
ϵ	30.71	1.08×10^{-11}

S3 Unraveling the free energy profile and its various contributions

In Figure S2a the free energy profile of the diffusion of one ethane guest molecule through the gate of ZIF-8 modeled with the Krokidas FF in the NPT regime is shown. The other parts of Figure S2 show various expansions of the free energy into enthalpy, covalent and non-bonding energy, as well as the 6MR ring gate size plot.

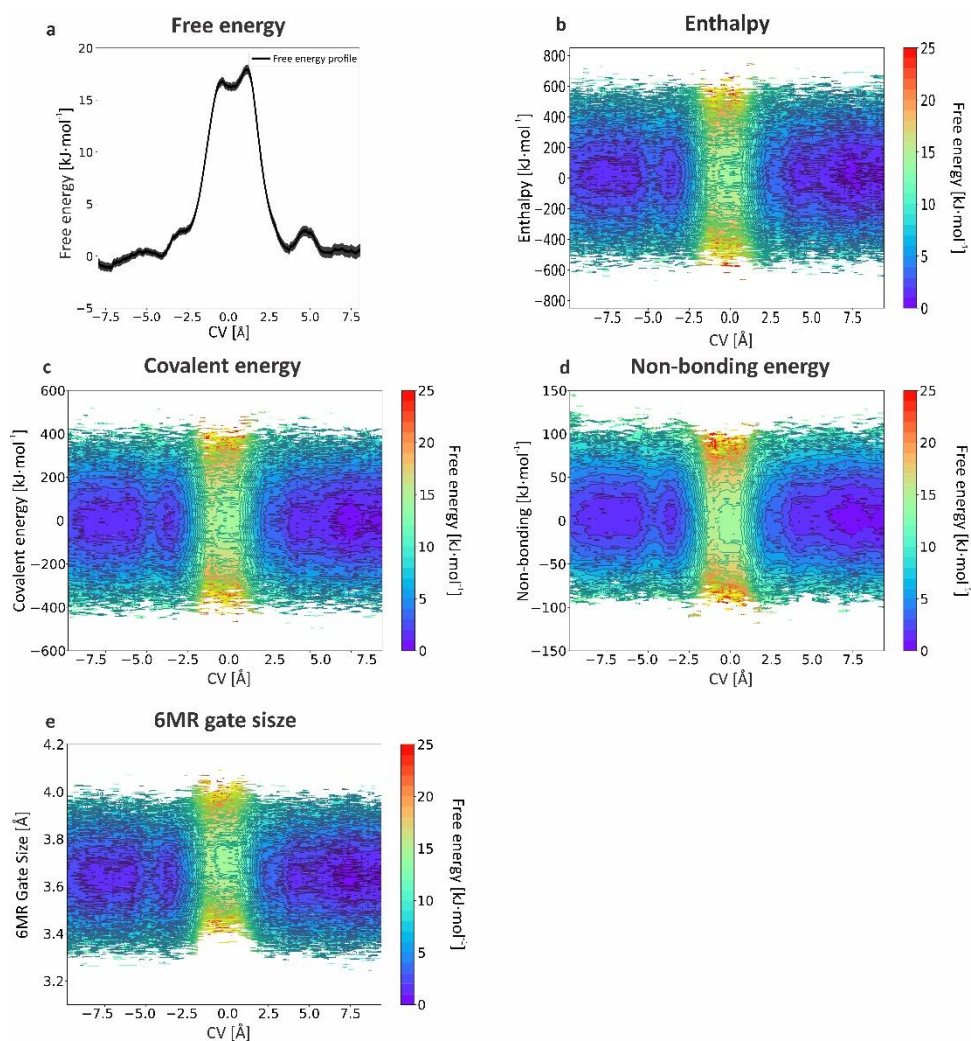


Figure S2: (a) Free energy profile of the diffusion of one ethane guest molecule in the ZIF-8 host structure simulated with the Krokidas FF in the NPT regime. (b) Two-dimensional enthalpy profile of the diffusion of ethane in ZIF-8. The reactant state is reference to 0 kJ/mol. (c) 2D plot of the covalent energy against the CV. The reactant state is referenced to 0 kJ/mol. (d) 2D plot of the non-bonding energy against the CV, with the reactant state being set to 0 kJ/mol. (e) 2D plot of the 6MR gate size of the ZIF-8 framework.

Figure S3 shows a 2D FES of the enthalpy of the diffusion of one ethane molecule in ZIF-8 and the corresponding sampling error profile. From the error profile it can be seen that the uncertainty of the free energy of the 2D profile is low. This means that the simulation sampled the phase space well and that only minimal variations in the 2D FES are expected between different trajectories.

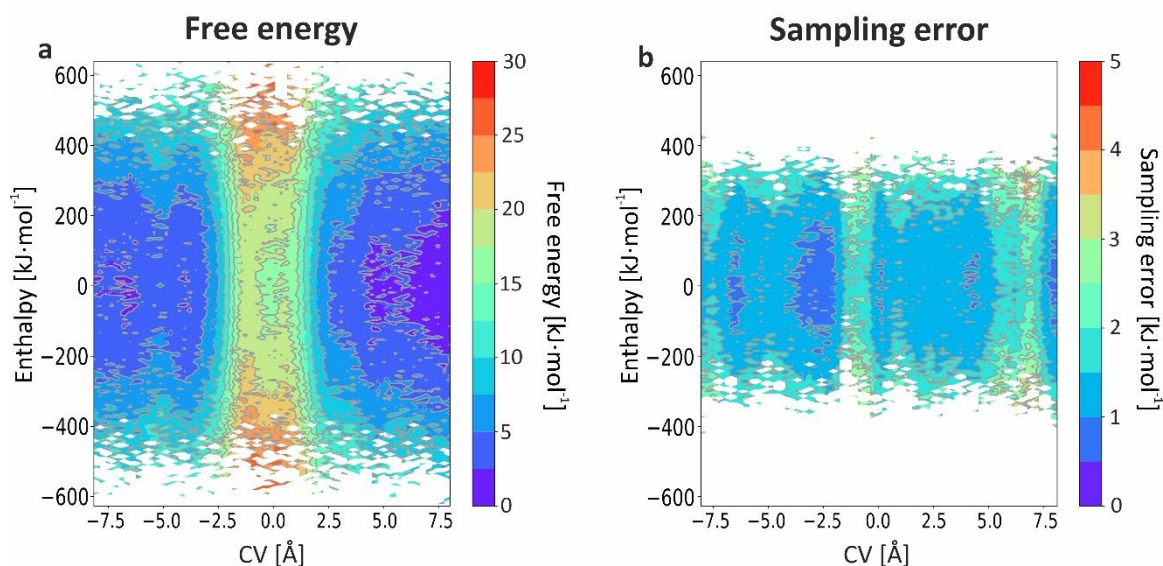


Figure 3: (a) 2D Free energy surface in terms of CV quantifying diffusion progress and total enthalpy of the system for the case of a single ethane molecule in ZIF-8 at 300 K and 1 bar. (b) Estimated sampling error on the FES expressed in (a).

In Figures S4a and S4b a schematic representation of the 6MR gate is shown. Figure S4b shows in detail the different components needed for the angular analysis of the MeIM linkers. The angle (α) of a MeIM linker is obtained at every step of the simulation trajectories as $\alpha = 90^\circ - \cos^{-1}\left(\frac{r_{6-Zn} - r_{6MR}}{l_{MeIM}}\right)$, where r_{6-Zn} is the radius of the ring spanned by the 6 Zn atoms, r_{6MR} is the radius of the ring spanned by the 3 MeIM linkers and l_{MeIM} is the length of the MeIM linker that is above the ring spanned by the 6 Zn atoms, as indicated in Figure S3b. This analysis is done for all three MeIM linkers separately and one representative 2D FES of one of the angles is shown in Figure S3c. An additional analysis of the other 3 MeIM linkers, which point towards the other side of the 6 Zn ring, is performed in the same way and the resulting 2D FES of one representative angle (β) is shown in Figure S3d.

The angle of the MeIM linkers forming the 6MR gate varies uniformly between -30° and 30° when the guest molecule is in the cages of ZIF-8, as can be seen from Figure S3c. When the guest molecule however enters the gate a minor increase in α of around 2° can be observed. This range of angles shows that the MeIM linkers can perform a two-site flip, where they change between the ZIF-8 cages they are pointing towards. This is similar to what the group of Kolokolov et al. measured, where they found that the MeIM linkers of the ZIF-8 structure at ambient pressure can occupy two separate directions with an angular difference of 34° between them, which fits within the range of angles of 40° seen in our simulations.² A difference between the computational and experimentally seen activation energy of the linker flip, can be due to multiple reasons, one of which is the level of theory or force field used for the simulations, which can have a significant impact on the framework

flexibility and gate size.³ Another reason is the loading of the system, where the loading of a specific guest molecule can change the behavior of the gate. In the case of ethane, it can be seen that the gate does open up to encompass the ethane guest molecule, however it is less obvious to recognize a direct impact of an ethane molecule entering the gate on the orientation of such an imidazole linker. In Figure S3d a representative angle of the other three MeIM linkers (β) is shown.

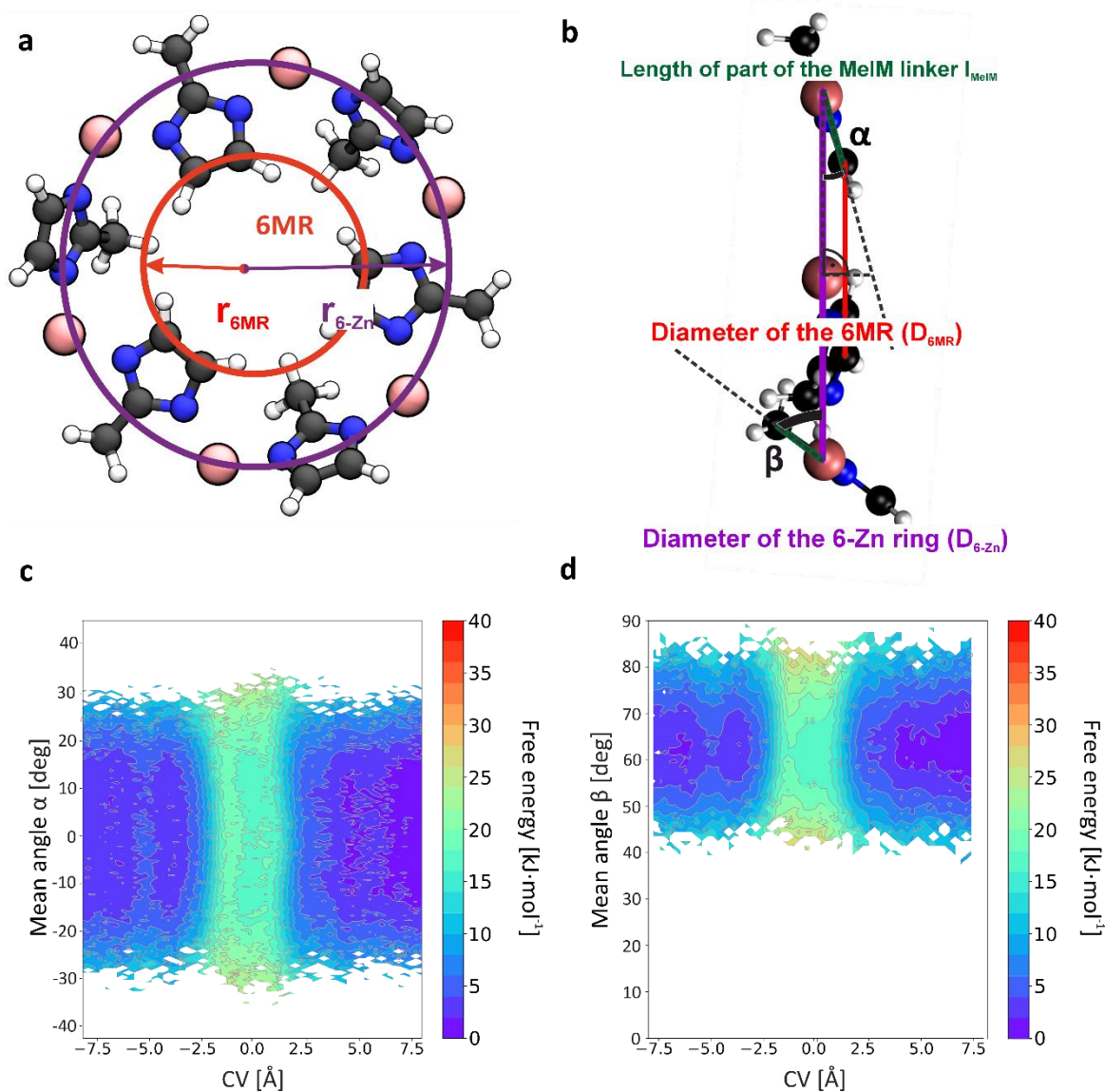


Figure S4: (a) Schematic representation of the gate connecting two ZIF-8 cages with indication of the 6MR gate in red and the 6-Zn ring in purple. Color code: Zn (pink), N (dark blue), C (dark grey) and H (white). (b) Schematic side view of parts of the gate with indication of the 6-Zn ring, 6MR and the angle α used for further investigation. Some of the MeIM linkers are removed for clarity in this figure. (c) 2D PES of the angle (α) of one of the 3 MeIM linkers indicated in (b). (d) 2D PES of the angle (β) of one of the MeIM linkers indicated in (b).

S4 Temperature dependence

In Figure S5a the free energy profiles of the ethane diffusion through ZIF-8 at different temperatures in terms of $k_B T$ are plotted. The results of the projection of enthalpy, 6MR ring gate size and volume plots are shown in Figure S5b to S5d. In the volume and gate size plots an impact of the temperature change can be seen. In Figure S9 a plot of the free energy barrier at different temperatures is shown. In Figure S10 a plot of the temperature dependent self-diffusion coefficient is shown. From this plot

an Arrhenius fit can be performed to extract the temperature independent activation energy of 2.1 kJ/mol and diffusion coefficient of $3.56 \times 10^{-10} \text{ m}^2/\text{s}$ of ethane diffusion in ZIF-8.

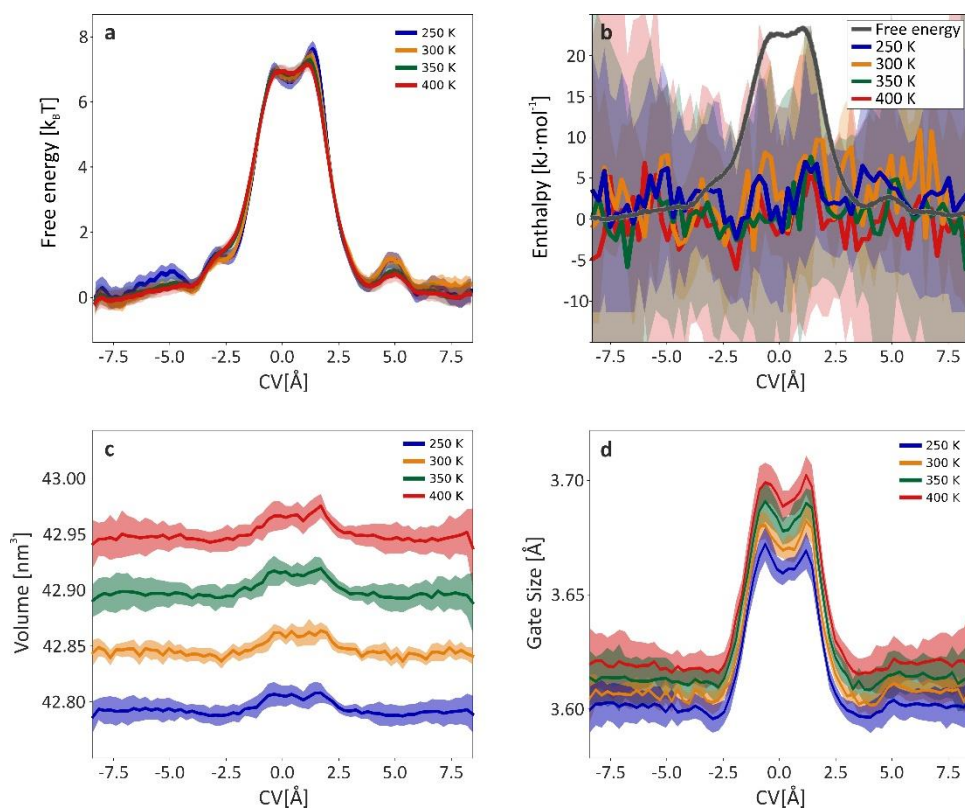


Figure S5: (a) Free energy profile of the diffusion of one ethane molecule in ZIF-8 in terms of $k_B T$, simulated at different temperatures. The simulation is a Krokidas et al. FF based umbrella simulation in the NPT regime. (b) Projected enthalpy profiles of the diffusion of one ethane guest molecule in ZIF-8 at different temperatures. The free energy profile of the diffusion at 300 K is plotted in grey. (c) Projected volume plots of the ethane diffusion in ZIF-8 at different temperatures. (d) Projected gate size plots of the ethane diffusion in ZIF-8 at different temperatures.

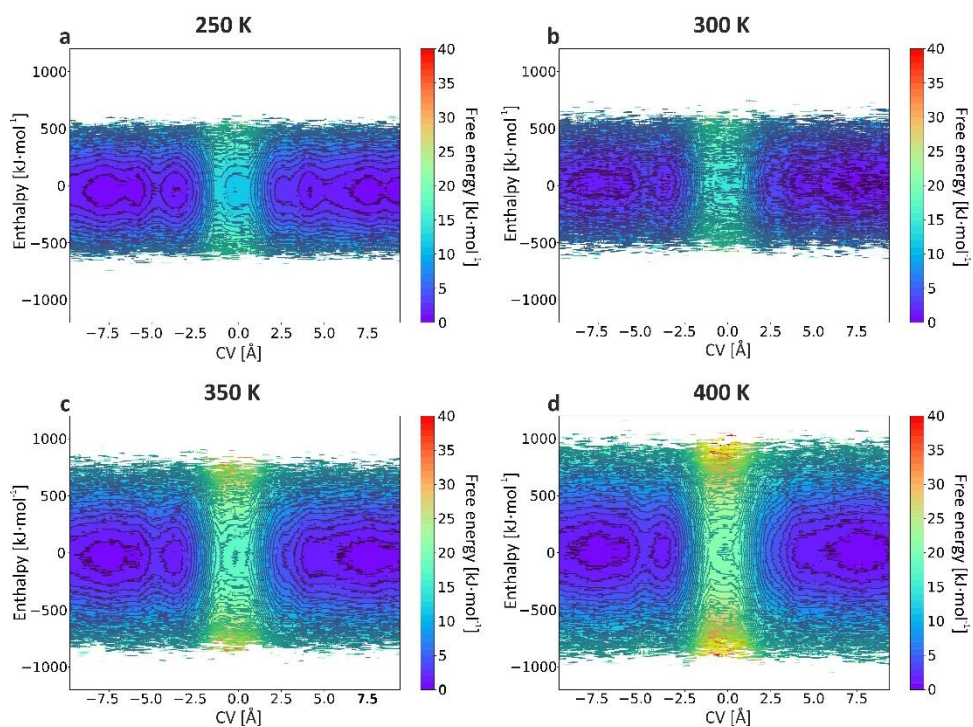


Figure S6: 2D enthalpy profiles at different temperatures for the diffusion of one ethane molecule through a ZIF-8 host structure. The simulations are performed with the Krokidas et al. FF in the NPT regime and the chosen temperatures are (a) 250 K, (b) 300 K, (c) 350 K and 400 K.

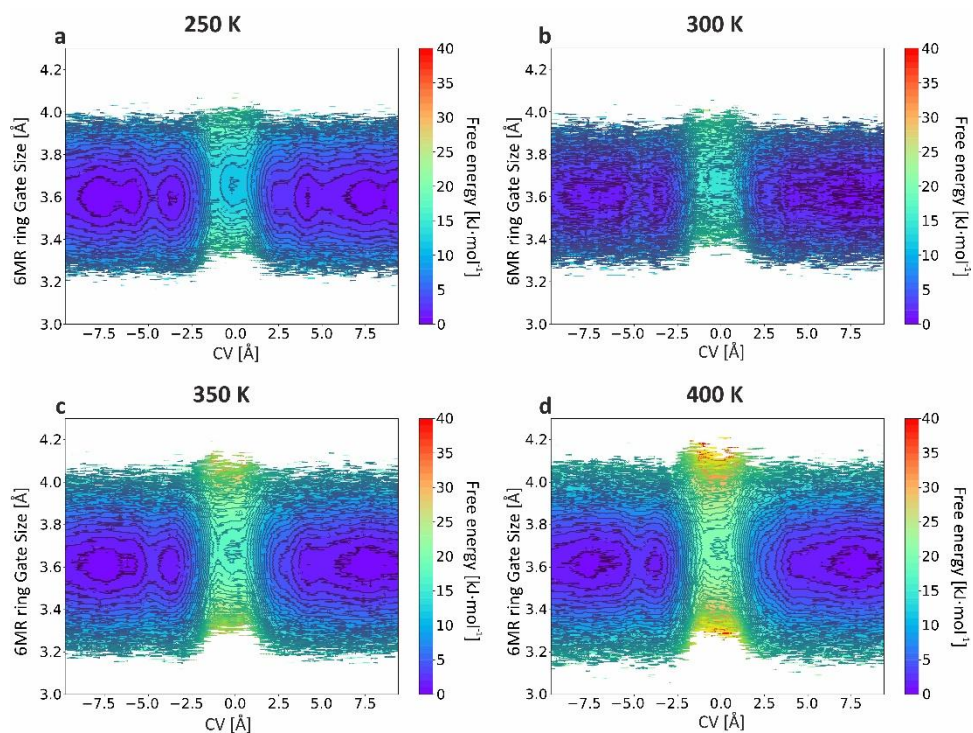


Figure S7: Gate size plot of the 6MR ring gate at different temperatures for the diffusion of one ethane molecule through a ZIF-8 host structure. The simulations are performed with the Krokidas et al. FF in the NPT regime and the chosen temperatures are (a) 250 K, (b) 300 K, (c) 350 K and 400 K.

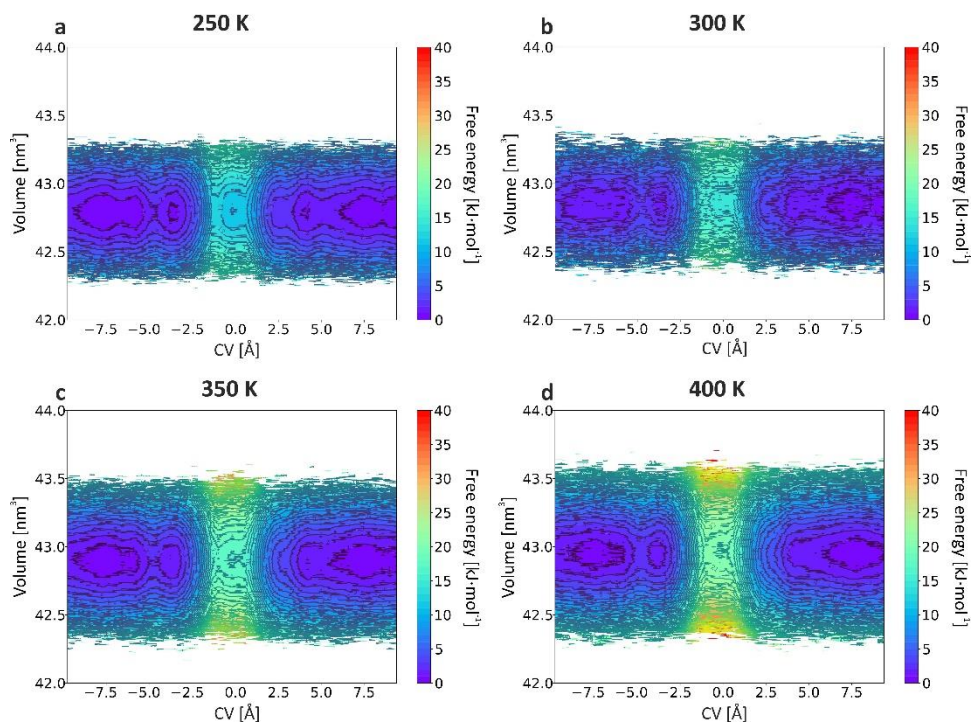


Figure S8: 2D volume plots at different temperatures for the diffusion of one ethane molecule through a ZIF-8 host structure. The simulations are performed with the Krokidas et al. FF in the NPT regime and the chosen temperatures are (a) 250 K, (b) 300 K, (c) 350 K and 400 K.

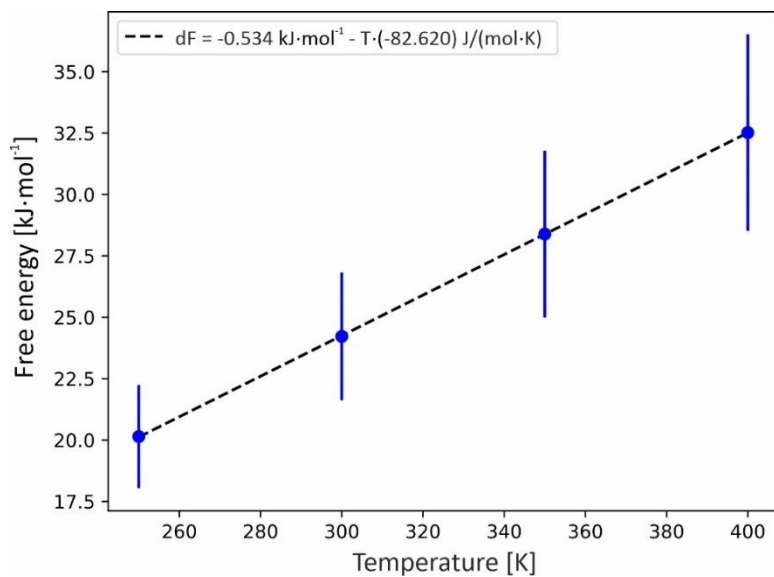


Figure S9: Plot of the free energy barrier of the diffusion of one ethane guest molecule in ZIF-8 at different temperatures with corresponding error bar. A linear fit of the free energy barriers results in $\Delta F = \Delta H - T \cdot \Delta S$ with $\Delta H \approx -1$ kJ/mol and $\Delta S \approx -83$ J/(mol.K).

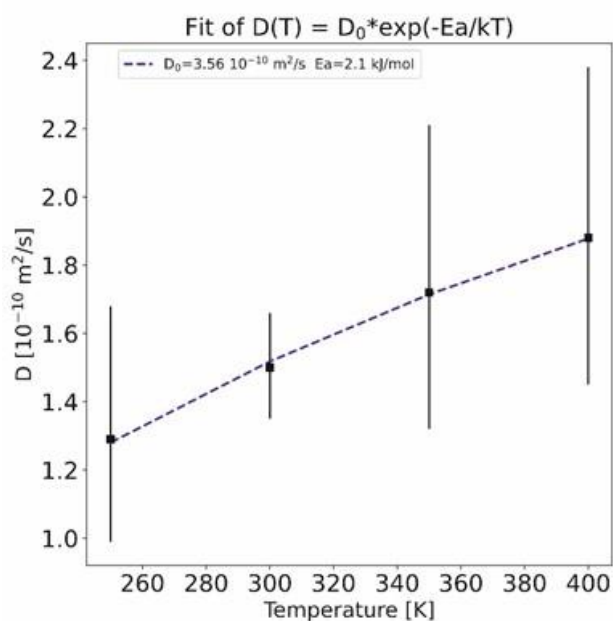


Figure 10: Self-diffusion coefficient of the diffusion of one ethane guest molecule in ZIF-8 at 1 bar as a function of temperature. An Arrhenius fit of the computed self-diffusion coefficients results in a temperature independent activation energy of 2.1 kJ/mol and diffusion coefficient of $3.56 \times 10^{-10} \text{ m}^2/\text{s}$.

S5 Loading dependence

The expansion and projection of the free energy profiles of the different loaded ZIF-8 host structure into multiple different second collective variables are shown in Figures S11 to S24. The loading of the ZIF-8 framework happens in the asymmetric case only in cage A and in the symmetric loading both cage B and A are loaded equally. The heading of the following plots composes of n_A+1-n_B with n_A being the loading of cage A and the the guest molecule and n_B being the loading of cage B.

S5.1 Asymmetric

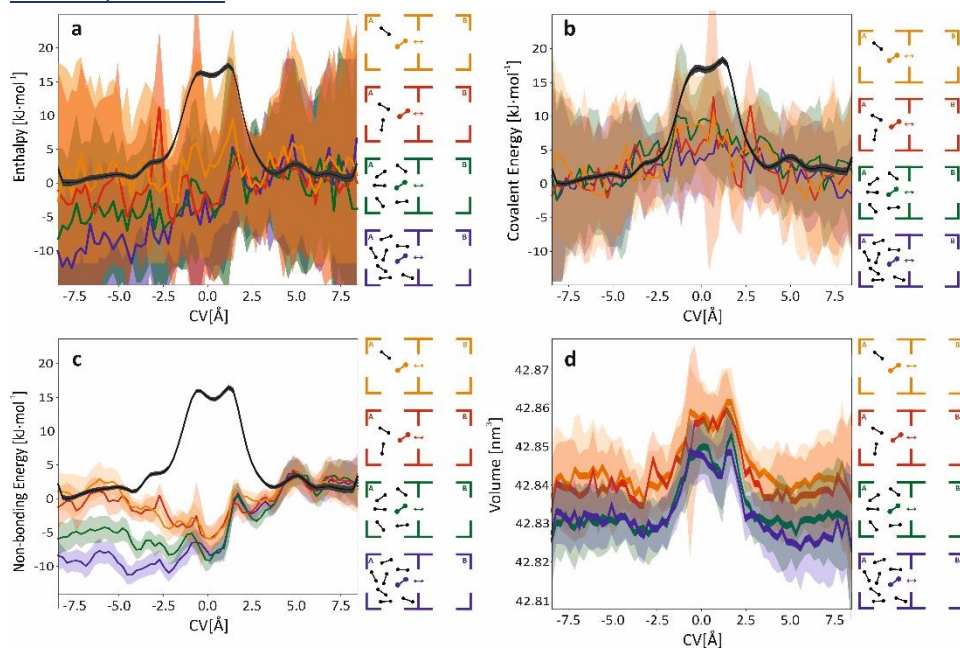


Figure S11: (a) Projected enthalpy profiles of the asymmetrically ethane loaded ZIF-8 structure. A reference free energy profile of the ethane diffusion in ZIF-8 is plotted in grey. (b) Projected covalent energy profile of the asymmetrically loaded

ZIF-8 structure. A reference free energy profile δ is plotted in grey. (c) Projected non-bonding energy profile of the diffusion of the asymmetrically loaded ZIF-8 structure. (d) Projected volume profiles of the asymmetrically loaded ZIF-8 structure.

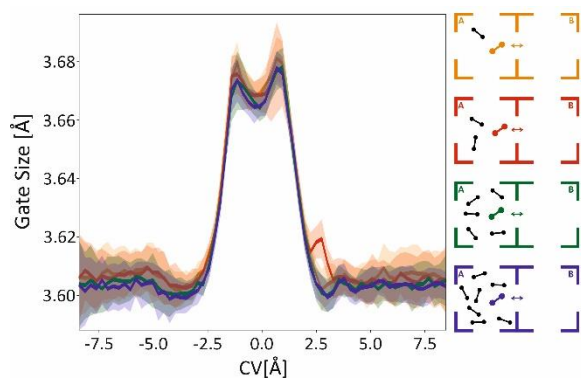


Figure S12: Projected 6MR ring gate size profiles of the diffusion of one ethane guest molecule in asymmetrically loaded ZIF-8.

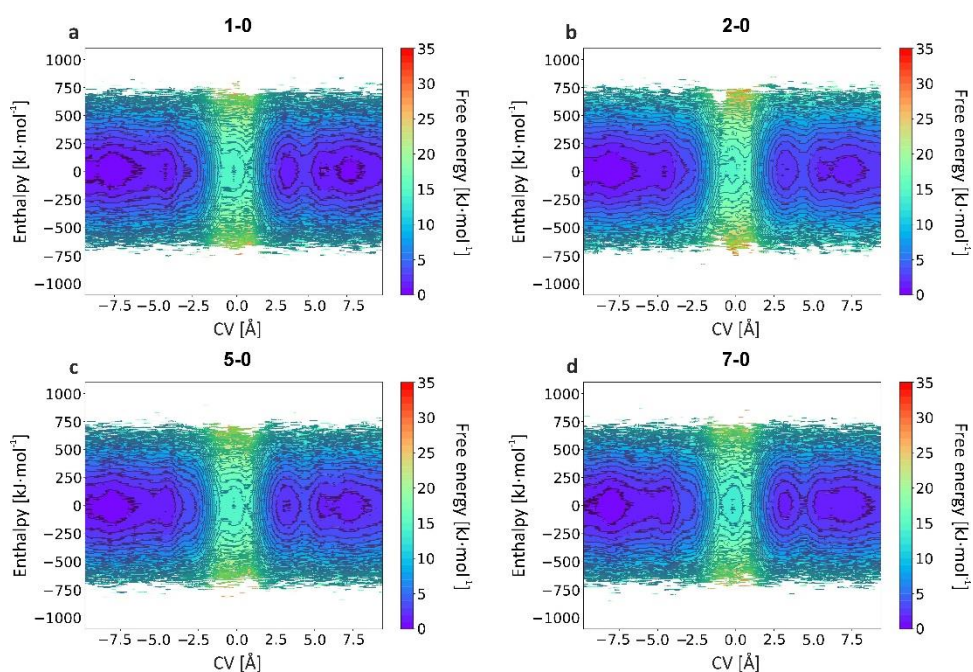


Figure S13: 2D enthalpy profiles at different loadings for the diffusion of one ethane molecule through a ZIF-8 host structure. The simulations are performed with the Krokidas et al. FF in the NPT regime. The loadings are (a) 1-0, (b) 2-0, (c) 5-0 and (d) 7-0.

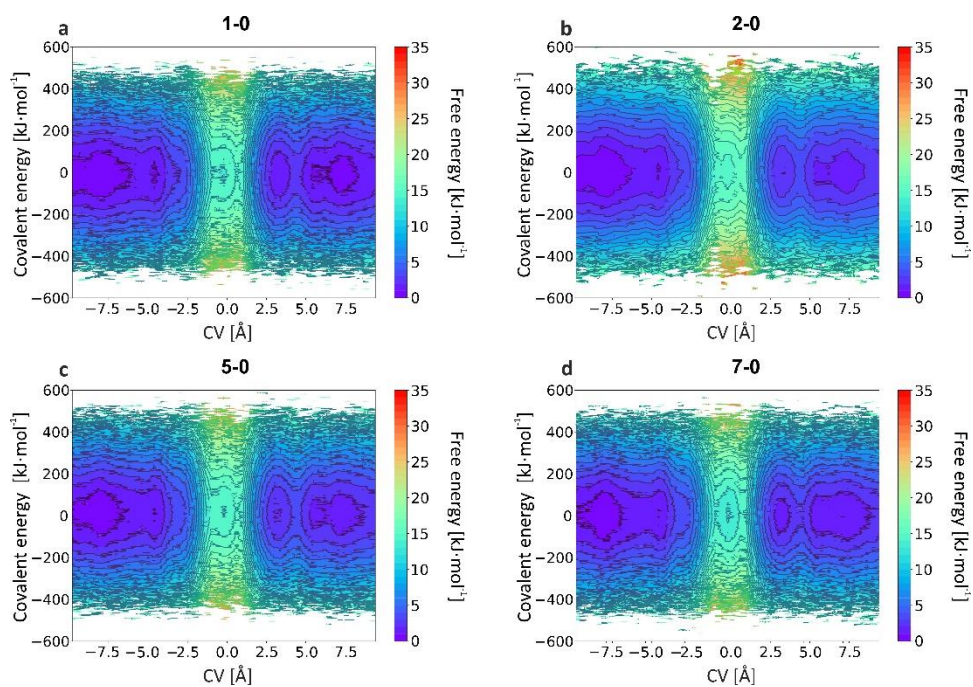


Figure S14: 2D covalent profiles at different loadings for the diffusion of one ethane molecule through a ZIF-8 host structure. The simulations are performed with the Krokidas et al. FF in the NPT regime. The loadings are (a) 1-0, (b) 2-0, (c) 5-0 and (d) 7-0.

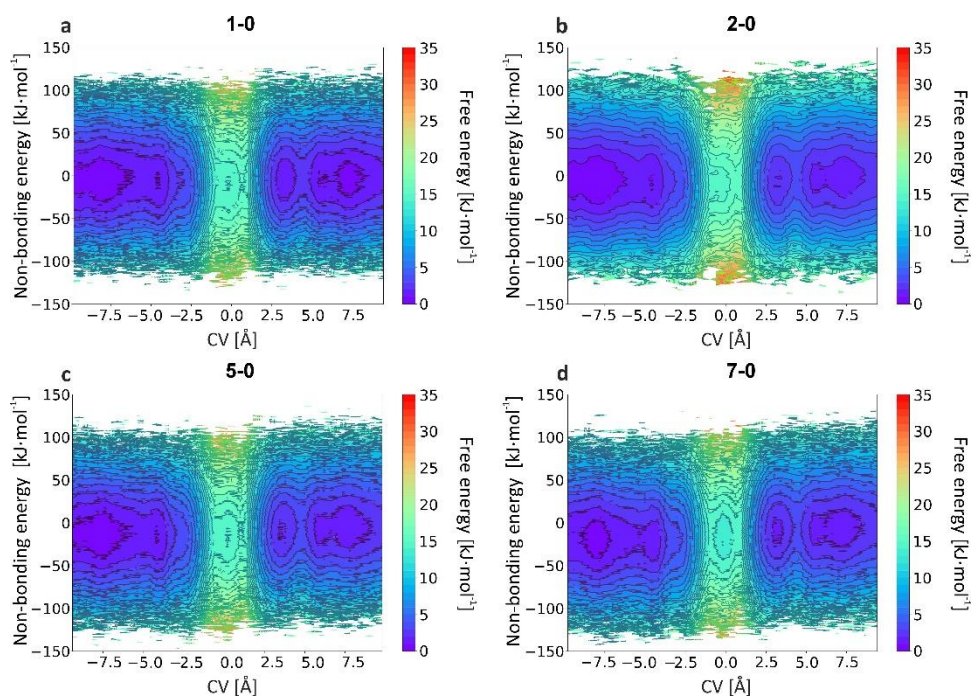


Figure S15: 2D non-bonding profiles at different loadings for the diffusion of one ethane molecule through a ZIF-8 host structure. The simulations are performed with the Krokidas et al. FF in the NPT regime. The loadings are (a) 1-0, (b) 2-0, (c) 5-0 and (d) 7-0.

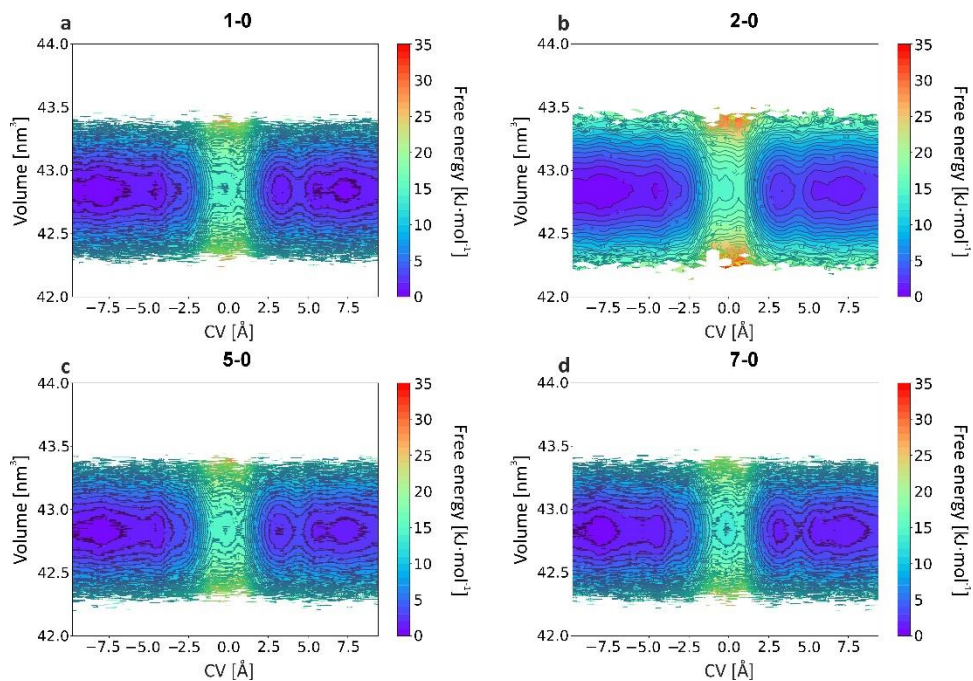


Figure S16: 2D volume profiles at different loadings for the diffusion of one ethane molecule through a ZIF-8 host structure. The simulations are performed with the Krokidas et al. FF in the NPT regime. The loadings are (a) 1-0, (b) 2-0, (c) 5-0 and (d) 7-0.

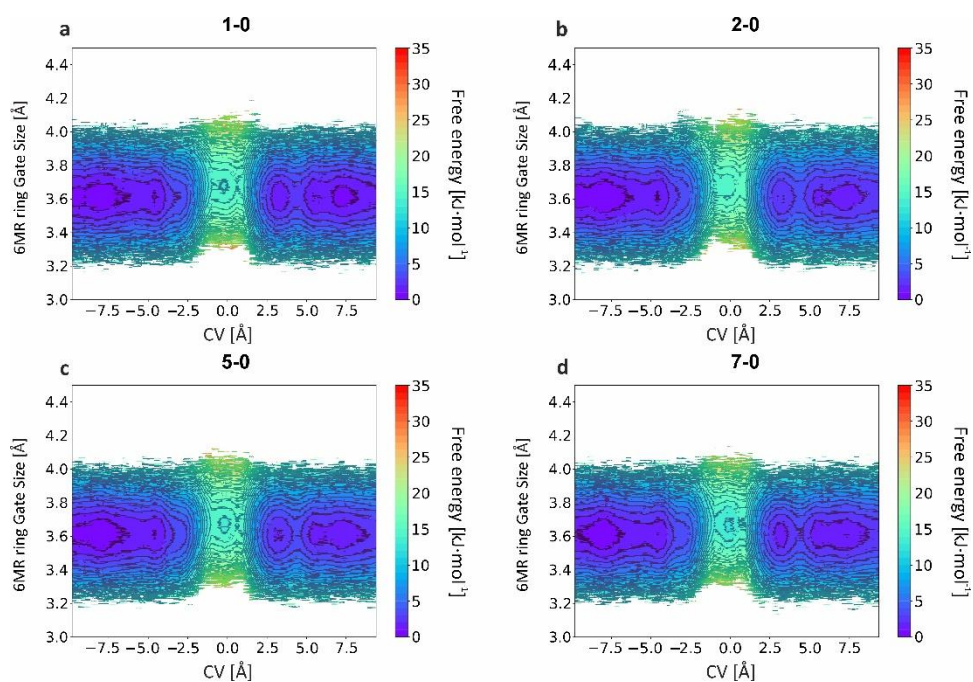


Figure S17: 6MR ring gate size profiles at different loadings for the diffusion of one ethane molecule through a ZIF-8 host structure. The simulations are performed with the Krokidas et al. FF in the NPT regime. The loadings are (a) 1-0, (b) 2-0, (c) 5-0 and (d) 7-0.

S5.2 Symmetric

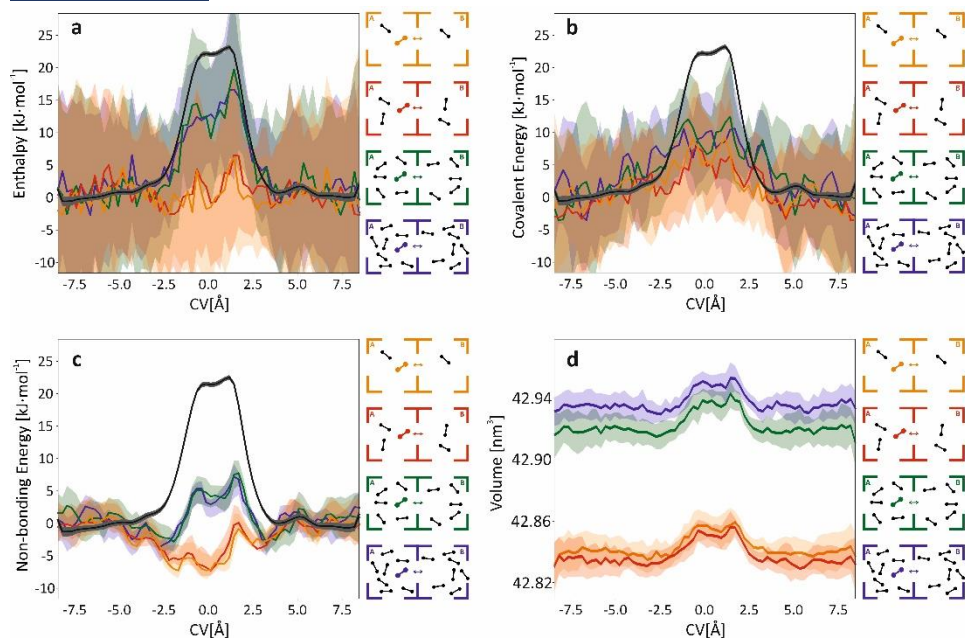


Figure S18: (a) Projected enthalpy profiles of the symmetrically ethane loaded ZIF-8 structure. A reference free energy profile of the ethane diffusion in ZIF-8 is plotted in grey. (b) Projected covalent energy profile of the symmetrically loaded ZIF-8 structure. A reference free energy profile is plotted in grey. (c) Projected non-bonding energy profile of the diffusion of the symmetrically loaded ZIF-8 structure. (d) Projected volume profiles of the symmetrically loaded ZIF-8 structure.

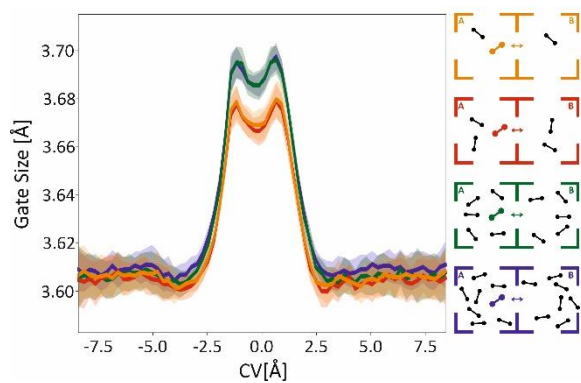


Figure S19: Projected 6MR ring gate size profiles of the diffusion of one ethane guest molecule in symmetrically loaded ZIF-8.

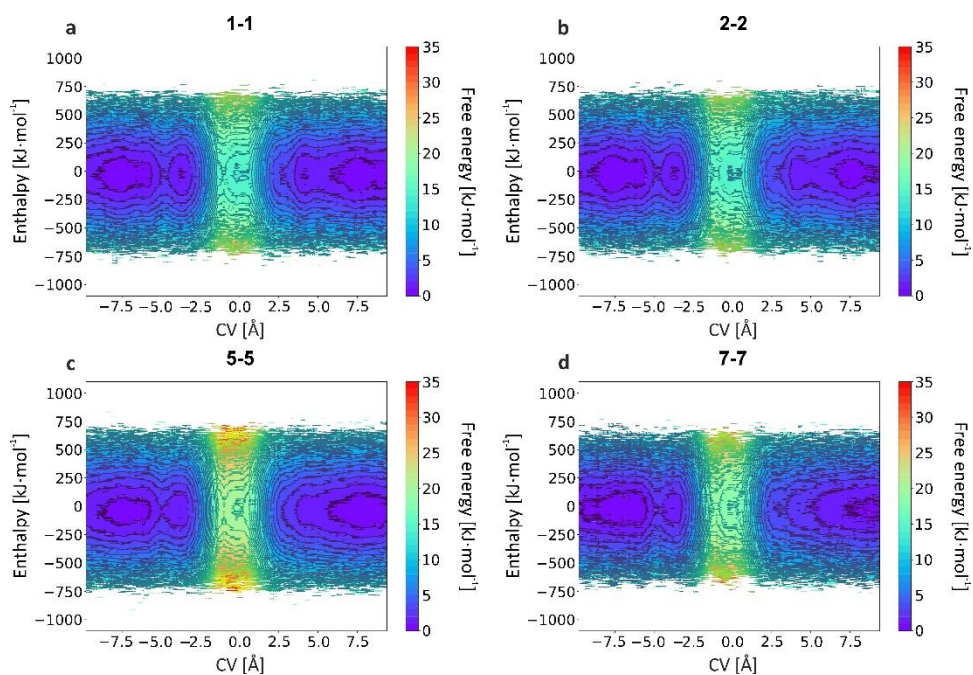


Figure S20: 2D enthalpy profiles at different loadings for the diffusion of one ethane molecule through a ZIF-8 host structure. The simulations are performed with the Krokidas et al. FF in the NPT regime. The loadings are (a) 1-0, (b) 2-0, (c) 5-0 and (d) 7-0.

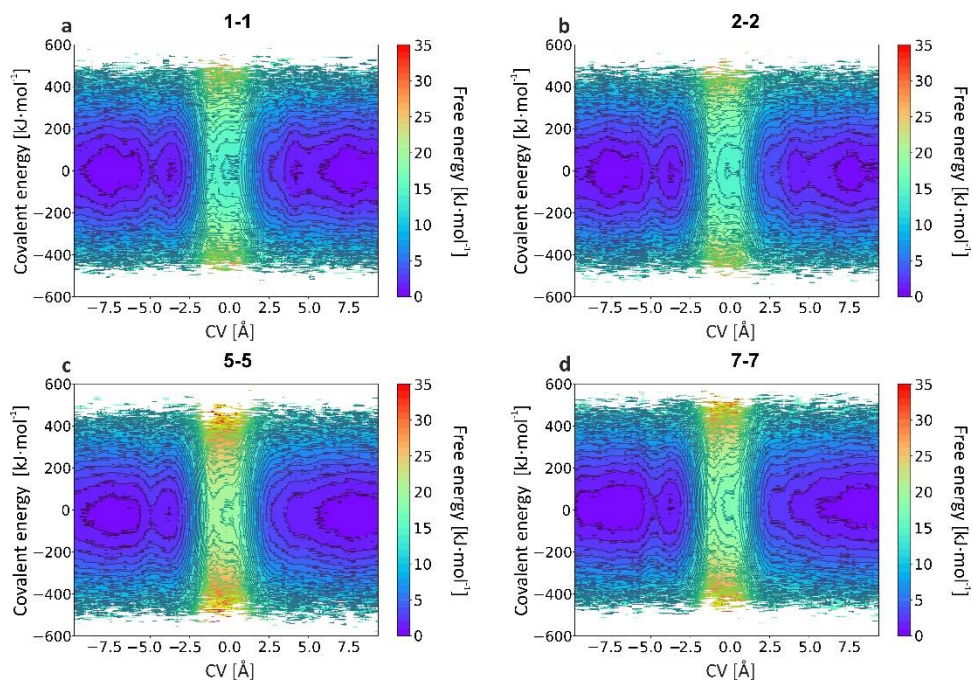


Figure S21: 2D covalent profiles at different loadings for the diffusion of one ethane molecule through a ZIF-8 host structure. The simulations are performed with the Krokidas et al. FF in the NPT regime. The loadings are (a) 1-0, (b) 2-0, (c) 5-0 and (d) 7-0.

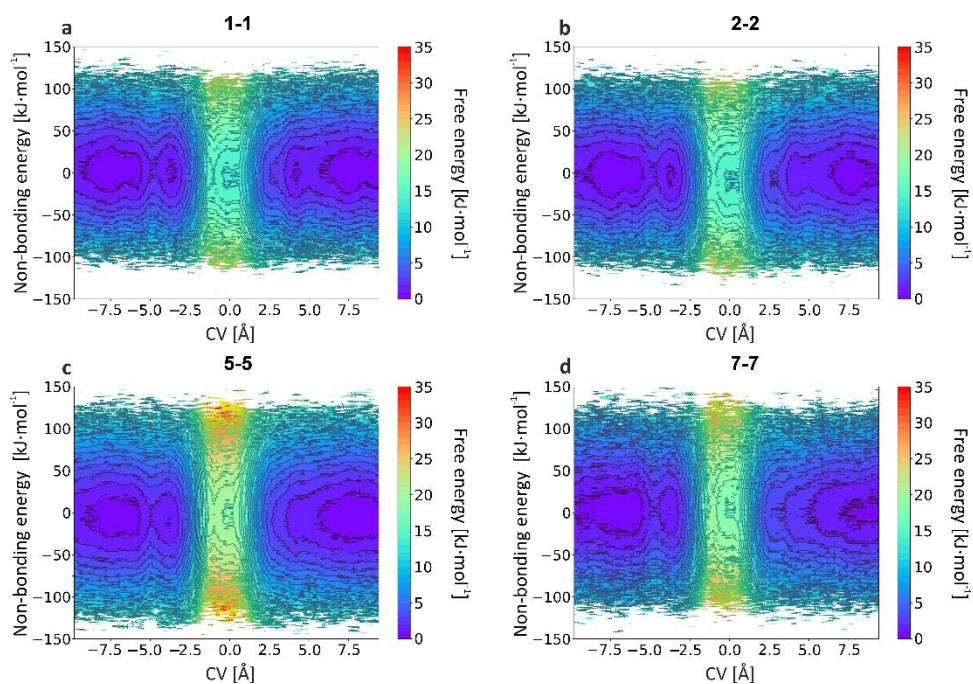


Figure S22: 2D non-bonding profiles at different loadings for the diffusion of one ethane molecule through a ZIF-8 host structure. The simulations are performed with the Krokidas et al. FF in the NPT regime. The loadings are (a) 1-0, (b) 2-0, (c) 5-0 and (d) 7-0.

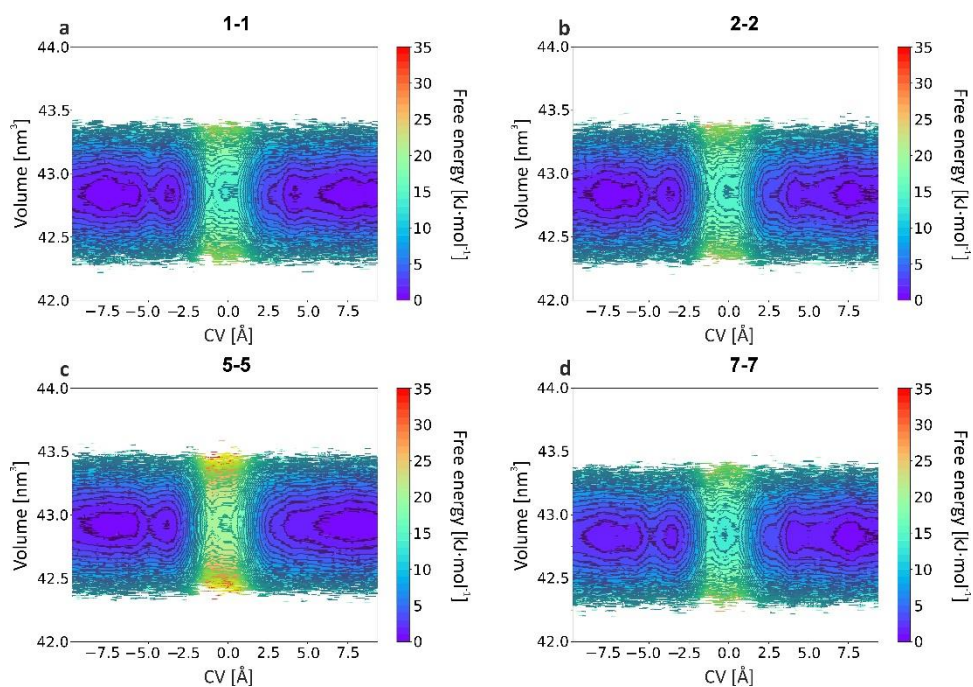


Figure S23: 2D volume profiles at different loadings for the diffusion of one ethane molecule through a ZIF-8 host structure. The simulations are performed with the Krokidas et al. FF in the NPT regime. The loadings are (a) 1-0, (b) 2-0, (c) 5-0 and (d) 7-0.

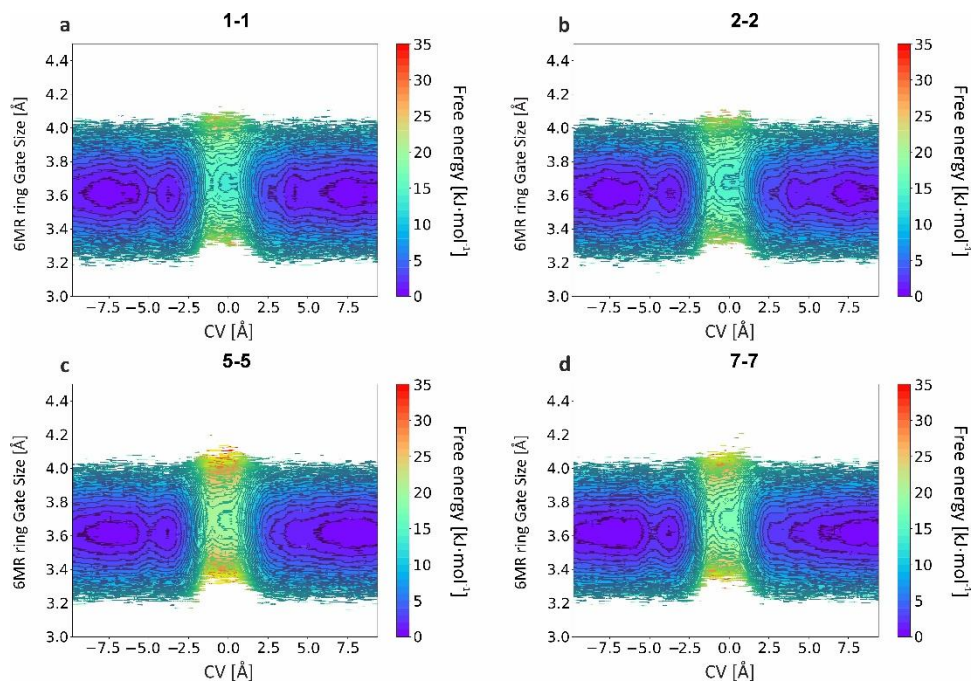


Figure S24: 6MR ring gate size profiles at different loadings for the diffusion of one ethane molecule through a ZIF-8 host structure. The simulations are performed with the Krokidas et al. FF in the NPT regime. The loadings are (a) 1-0, (b) 2-0, (c) 5-0 and (d) 7-0.

■ REFERENCES

- (1) Krokidas, P.; Moncho, S.; Brothers, E. N.; Castier, M.; Jeong, H.-K.; Economou, I. G. On the Efficient Separation of Gas Mixtures with the Mixed-Linker Zeolitic-Imidazolate Framework-7-8. *ACS Appl. Mater. Interfaces* **2018**, *10* (46), 39631–39644. <https://doi.org/10.1021/acsami.8b12605>.
- (2) Kolokolov, D. I.; Stepanov, A. G.; Jobic, H. Mobility of the 2-Methylimidazolate Linkers in ZIF-8 Probed by 2H NMR: Saloon Doors for the Guests. *J. Phys. Chem. C* **2015**, *119* (49), 27512–27520. <https://doi.org/10.1021/acs.jpcc.5b09312>.
- (3) Zheng, B.; Maurin, G. Mechanical Control of the Kinetic Propylene/Propane Separation by Zeolitic Imidazolate Framework-8. *Angewandte Chemie International Edition* **2019**, *58* (39), 13734–13738. <https://doi.org/10.1002/anie.201906245>.